Impact Factor 0.7
Q3

Journal of
Research in Pharmacy

Research Article

www.jrespharm.com

Identification of potential antidiabetic inhibitor from *Mimosa pudica* Linn. through *in silico* molecular modeling and DFT tools

Chandrasekar PALANİCHAMY [1], Pavadai PARASURAMAN [2], Panneerselvam THEİVENDREN[3], Madasamy SUNDAR [1], Alagarsamy SANTHANA KRİSHNA KUMAR[4], Selvaraj KUNJİAPPAN[1]*

1. Department of Biotechnology, Kalasalingam Academy of Research and Education, Krishnankoil-626126, Tamilnadu. India.
2. Department of Pharmaceutical Chemistry, Faculty of Pharmacy, M.S. Ramaiah University of Applied Sciences, Bengaluru-560054, Karnataka, India.
3. Department of Pharmaceutical Chemistry & Analysis, School of Pharmaceutical Sciences, Vels Institute of Science, Technology & Advanced Studies, Pallavaram, Chennai-600117, Tamil Nadu, India.
4. Department of Chemistry, National Sun Yat-sen University, No. 70, Lienhai Road, Gushan District, Kaohsiung 80424, Taiwan.

* Corresponding Author. E-mail: selvaraj.k@klu.ac.in (S.K.); Phone: +91-9994972108.

Received: 12 July 2024 / Revised: 19 August 2024 / Accepted: 22 August 2024

ABSTRACT: Presently prescribed synthetic antidiabetic drugs effectively manage type 2 diabetes mellitus (T2DM) and, at the same time, cause severe toxic side effects. Generating novel molecules is significantly hampered by their longer time and insufficient physicochemical, pharmacokinetic, and intrinsic properties. In this view, a potential antidiabetic inhibitor from *Mimosa pudica* L. can be identified via *in silico* molecular modeling and Density Functional Theory (DFT) tools for effi-ciently managing T2DM with minimal side effects. Primarily, we evaluated the network analysis to observe the genes, proteins, and enzymes contributing to the signaling network of Peroxisome proliferator-activated receptors (PPARs) family proteins and identified PPARγ as a potential antidiabetic receptor protein. Thirty-six bioactive molecules were picked from *M. pudica* L. ethanolic extract through LC-MS and GC-MS analysis of our previous study report. Based on the pilot study, the selected molecule's structure was drawn using Chemsketch software and docked against the PPARγ receptor. Interestingly, three high-scoring molecules were observed, namely, apigetrin (-8.6 kcal/mol), orientin (-8.5 kcal/mol), isoquercetin (-8.3 kcal/mol), whereas compared to standard reference drug pioglitazone (-8.3 kcal/mol). In addition, molecular dynamics (MD) simulation research to discover intermolecular interactions and the stability of protein-ligand complexes. The *in silico* ADME&T studies displayed that apigetrin showed drug-like behaviours and less toxic effects. Further, MD simulation studies established the stability of apigetrin and orientin with the PPARγ protein binding pockets. According to these discoveries, the top-scored molecule, apigetrin, might be used as a potential antidiabetic inhibitor and can be used as a new optional medicine for the therapy of T2DM.

KEYWORDS: Type 2 diabetes mellitus; antidiabetic inhibitor; *Mimosa pudica* Linn.; molecular modelling tools

1. INTRODUCTION

Diabetes mellitus has become a significant health concern across the world [1]. Type 2 diabetes mellitus (T2DM) is an endocrine-cum-vascular condition in which the body generates insufficient or inefficient insulin, resulting in an excess of glucose in the circu-latory system [2]. It is a progressive disorder frequently connected with dyslipidemia, obe-sity, and high blood pressure. It is more common among overweight and obese adults in their middle to late years, but it can also affect younger people and those with a lower body mass index (BMI) [3]. According to the statistical report, 77 million people in India had diabetes in 2019, the number is anticipated to climb to 134 million by 2045 [4]. In addition, the expanding affliction of T2DM was usually assumed to impact adult populations, however it impacts victims from a young age of growth [5]. There is no remedy for T2DM liberation, although lifestyle modifications such as dietary changes, physical activity, weight control, and oral antihyperglycemic medicines can manage or postpone it [6]. T2DM, if not managed, can lead to renal failure, cardiovascular disease, stroke, lower limb amputa-tion, sexual dysfunction, and diabetic retinopathy [7]. Recently, many efforts have been made to increase the knowledge and awareness of T2DM management and risk factors, but still, morbidity and death

How to cite this article: Palanichamy C, Parasuraman P, Theivendren P, Sundar M, Santhana Krishna Kumar A, Kunjiappan S. Identification of potential antidiabetic inhibitor from Mimosa pudica Linn. through in silico molecular modeling and DFT tools. J Res Pharm. 2025; 29(4): 1468-1484.

https://dx.doi.org/10.29228/jrp.2022.00
ISSN: 2630-6344

rates have continued to rise internationally. The increasing prevalence of diabetes highlights the limitations of currently available pharmaceuticals, underlining the necessity for more alternative therapies to improve current treatments.

Many oral antihyperglycemic agents have recently been used to treat T2DM, with multiple modes of action producing various physiological functions; they either increase or decrease drug receptor regulation to improve insulin sensitivity, over-produced insulin secretion, or enhance glucose uptake in liver and muscle cells. However, the existing drugs are ineffective and poorly tolerated, resulting in mechanism-based adverse side effects such as hypoglycemia, overweight, and gastrointestinal issues [8]. In the late stages of T2DM, monotherapy or single-target drugs are unsuccessful; combination drug therapy with two or more oral antihyperglycemic agents from distinct classes that target several pathways may be needed for effective control [9]. On the other hand, the cost of synthetic medicines is gradually rising, and patients are denied access to cost-effective treatment alternatives, making diabetes more difficult to manage, especially in developing nations. Because diabetes necessitates long-term treatment, there is always a high demand for safe and affordable antidiabetic medication. As a result, researching and creating a target-specific medicine with minimal side effects may be the most successful method for improving diabetes therapy.

T2DM is mainly caused by insulin inefficient and insulin insufficiency due to alteration of lipid metabolism and pancreatic β cell damage [10]. Chronic inflammation, sleep abnormality, incretin dysregulation, hyperglucagonemia, amino acid metabolism, lipolysis, central appetite dysregulation, aberrant gastric emptying, gut dysbiosis, and islet amyloid polypeptide (IAPP) accumulation are all considered significant regulators in the pathogenesis of T2DM [11]. Their diversified combination increases the complexity and diversity of the patient's circumstances. In general, T2DM has been connected to many genes, enzymes, and proteins and their signaling pathways, identified as possible therapeutic targets for diabetic complications [5]. In this scenario, a graph theoretical network study is anticipated for metabolic networks encompassing receptor (enzymes, genes, and proteins) and synergistic ligand binding to active drugs [12]. Graph theoretical network analysis was employed to identify optimal targets for efficient glucose uptake in cells [13]. The graph theoretical network revealed PPARγ as a promising pharmaceutical target for con-trolling T2DM. PPARγ has essential roles in metabolism, including glucose homeostasis, which is disrupted in type 2 diabetes. PPARγ regulates adipogenesis in white adipose tissue, driving fibroblastic progenitors to adipocytes [14]. Medicinal plants and their secondary metabolites have been historically identified as an effective therapy for T2DM.

Mimosa pudica Linn. (Family: Mimosaceae) is a sub-woody plant, either annual or biannual, native to South America, also observed in Australia and India. The crude extract of *M. pudica* L. has traditionally been used to treat various health issues, including diabetes and cardiovascular disease [15]. The results of our previous study demonstrated that the ethanolic extract of *M. pudica* L. enhances the aphrodisiac behaviors of diabetic-induced male Wister rats and reduces the level of glucose in the circulatory system [16]. Therefore, we selected *M. pudica* L., plant and their active molecules presence in the extract. This work aimed to predict novel antidiabetic molecules from *M. pudica* L. via molecular modeling. Further, the pharmacokinetic and physicochemical properties of the observed active ingredients were considered. Molecular dynamics (MD) simulation experiments performed to confirm the stability of molecule complex and their efficiency of intermolecular interactions between chosen active molecules and the PPARγ protein.

2. RESULTS AND DISCUSSION

2.1. Graph theory

This study recreated the peroxisome proliferator-activated receptor (PPAR) signalling network as a graph, which contained multiple components such as genes, proteins (nodes), and interactions (edges). The network has 57 nodes with 70 edges, as shown in Figure 1 and Table 1. The measured values of degree (20), eccentricity (1), eigenvector (-0.3776), radiality (3.3393), and stress (171) were utilized to determine the starting point of the measurements and identify crucial nodes in the network structure. PPARγ was discovered as a potential therapeutic target due to its centrality and threshold values.

2.2. Active molecules

Based on our prior research findings, we found thirty-six bioactive compound molecules from the target plant *M. pudica* L. and the reference drug (pioglitazone), were chosen and optimized against several antidiabetic protein inhibitors. The *in silico* molecular docking studies using the optimized structures were performed against several antidiabetic protein inhibitors, with the results displayed in Table 2.

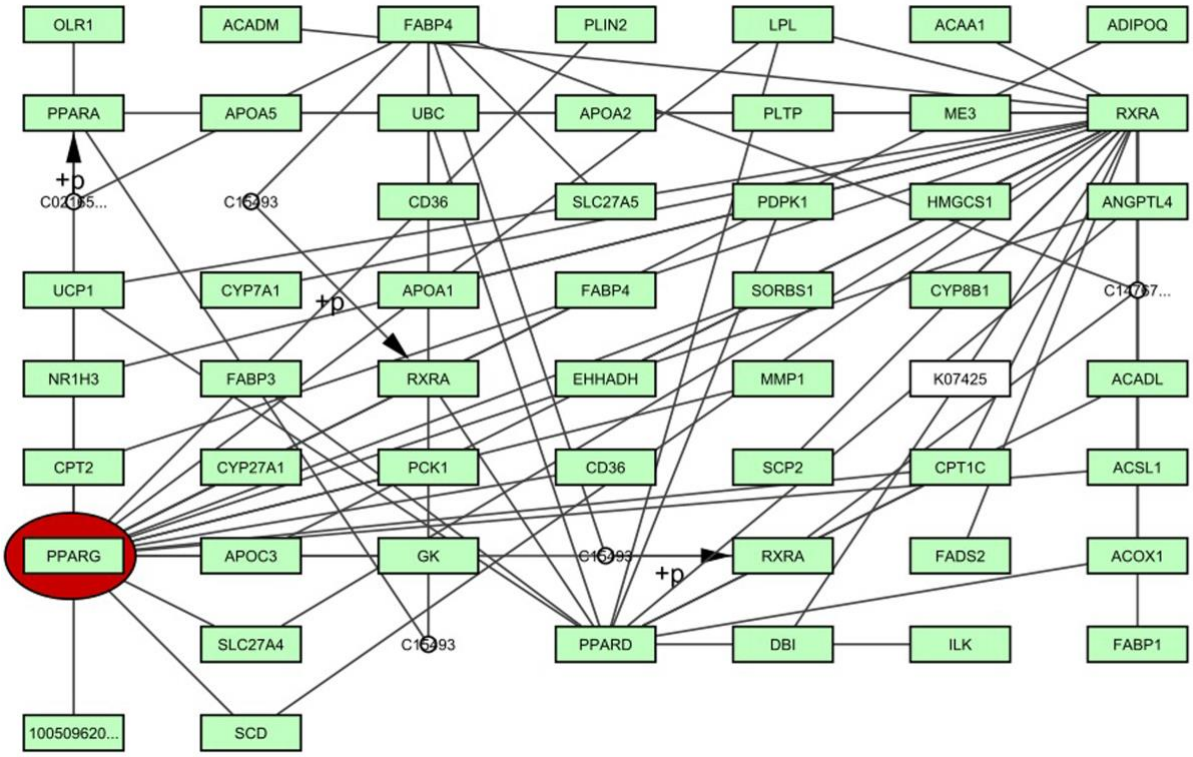

Figure 1. The signaling pathway of PPARγ.

Table 1. The results of threshold parameter values of the PPARγ network analysis.

Gene	Betweenness	Centroid	Closeness	Degree	Eccentricity	EigenVector	Radiality	Stress
PPARG	100.8	-19	19	20	1	-0.3776	3.339286	171
PPARD	38.4	-10	10	11	1	-0.1885	2.964286	50
FABP4	98	-49	15	7	0.25	-0.0141	2.160714	230
PPARA	119	-27	14	3	0.5	-0.1039	2.892857	216
RXRA	86.8	-20	10.5	3	0.5	-0.0696	2.714286	160
CPT1C	0	0	0	3	0	-0.194	3.410714	0
LPL	0	0	0	3	0	-0.194	3.410714	0
ANGPTL4	0	0	0	3	0	-0.194	3.464286	0
UCP1	0	0	0	3	0	-0.19399	3.410714	0
C02165	34	-28	10.17	2	0.33	-0.0202	2.267857	84
C15493	34	-28	10.17	2	0.33	-0.0202	2.321429	84
C15493	24	-21	7.83	2	0.33	-0.0143	2.053571	63
RXRA	32.4	-11	6	2	0.5	-0.0337	2.392857	44
ACSL1	0	0	0	2	0	-0.097	3.196429	0
SLC27A4	0	0	0	2	0	-0.162	3.214286	0
ACOX1	0	0	0	2	0	-0.129	2.946429	0
C14767	24	-21	7.83	2	0.33	-0.014	2	63
C15493	22	-12	4.83	2	0.33	-0.008	1.678571	36
SCD	0	0	0	2	0	-0.1617	3.196429	0
NR1H3	0	0	0	2	0	-0.1617	3.178571	0
CD36	0	-50	12.07	1	0.2	-0.0024	1.303571	0
SLC27A5	0	-50	12.07	1	0.2	-0.0024	1.285714	0

2.3. Binding pocket identification

The selected active molecules were subjected to structure-based molecular screening utilizing the antidiabetic protein binding pockets that had previously been studied. In molecular docking experiments, the receptor grid box led to more precise ligand posture scoring. The grid box was created to fit the surroundings of the first binding pockets. Figure 2 depicts PPARγ (PDB id: 5Y2O) with six binding pockets for ligand targeting. The binding packets were projected to be different colors. The first binding pocket (red color) has the most incredible score, with a pocket value of 20.94, 30 amino acid residues, and a probability binding score of 0.849.

Table 2. Bioactive molecules in the ethanolic extract of *Mimosa pudica* L. and their binding affinity against PPARγ protein.

CID	Molecules	PPARγ (PDB id: 5Y2O) kcal/mol
5280794	Stigmasterol	-7.8
114776	Isoorientin	-7.8
5280441	Vitexin	-7.9
70698280	Cassiaoccidentalin B	-8.2
162350	Isovitexin	-8.0
5280704	Apigetrin	-8.6
5280804	Isoquercetin	-8.3
5490064	Avicularin	-7.5
222284	Beta-Sitosterol	-7.5
5281679	Methyl quercetin	-7.3
5281675	Orientin	-8.5
64971	Betulinic acid	-7.9
5375199	Abscisic acid	-6.0
20061	Dibenzo[b,d]furan-3-amine	-6.5
5281166	Jasmonic acid	-5.6
5282796	Isolinoleic acid	-6.6
370	Gallic acid	-5.4
1153	DL-Tyrosine	-6.0
440473	L-Mimosine	-5.7
5282761	cis-vaccenic acid	-5.9
94715	Glucopyranuronic Acid	-5.4
164619	D-Pinitol	-4.4
190359	Mimosinic acid	-5.7
951	dl-Norepinephrine	-5.6
125409	Beta-D-Xylopyranose	-4.8
548229	3,4-Altrosan	-5.2
99057	2-Methoxyoxane-3,4,5-triol	-5.0
2519	Caffeine	-5.3
14080	1H-Imidazole-4-carboxylic acid	-4.6
241738	6,8-Dioxabicyclo[3.2.1]octane	-5.1
237332	5-Hydroxymethylfurfural	-5.2
7768	Azepan-2-one	-4.4
7968	4H-Pyran-4-One	-4.4
795	1H-Imidazole	-3.4
6341	Ethanamine	-2.4
5280489	Beta-carotene	-6.5
4829	Pioglitazone	-8.3

2.4. Structure-based screening

The structure-based screening approach investigated the intermolecular interactions of the chosen active molecules with potential antidiabetic receptor protein. The PyRx virtual tool in the AutoDock Vina program assessed the efficiency of thirty-six selected active compounds and reference ligands against a putative antidiabetic receptor protein (PPARγ). Three compounds with the highest binding scores against antidiabetic receptor protein was chosen for additional MD simulation investigations. Table 2 shows that the binding affinity of active molecules ranges from -2.30 to -8.60 kcal/mol.

2.5. Intermolecular interaction of antidiabetic receptor-ligand

The protein-ligand interaction profiler (PLIP) displayed the interactions between antidiabetic receptor protein and top-scored/reference ligands. Most active molecules had higher binding efficacies (-

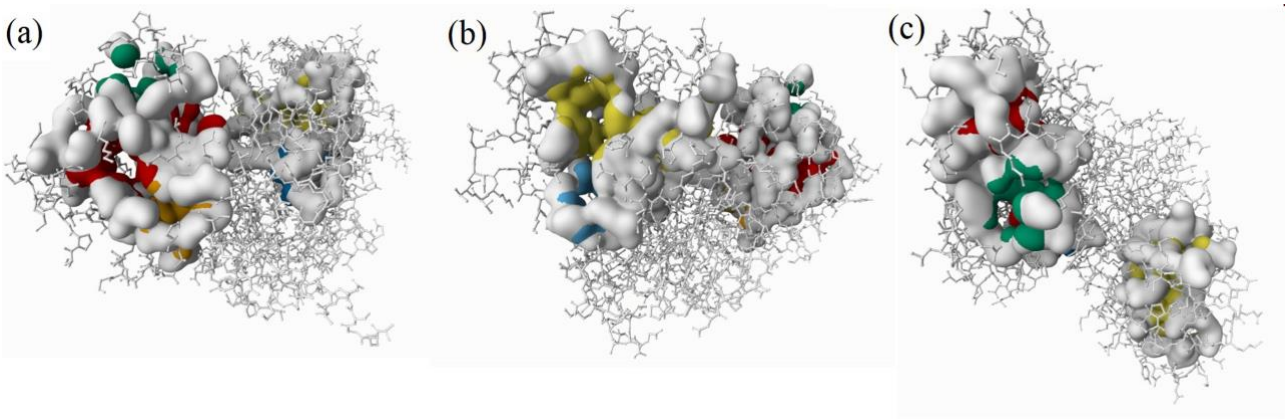

Figure 2. The PrankWeb tool is used to predict the binding pockets and correspondence binding sites of the PPARγ. Six binding pockets were predicted with different colors (red, light yellow, dark yellow, light blue, green, and dark blue). The first pocket is colored in red with a pocket score of 20.94, 30 amino acids, and a probability score of 0.849 (a). The second pocket is in light yellow, with a pocket score of 16.92, 29 amino acids, and a probability score of 0.790 (b). The third pocket is in dark yellow with a pocket score of 3.33, 12 amino acids, and a probability score of 0.121 (c). The fourth pocket is in light blue with a pocket score of 2.88, 10 amino acids, and a probability score of 0.092 (c). The fifth pocket is in green with a pocket score of 2.15, 11 amino acids, and a probability score of 0.050 (c), and the six pocket is in dark blue with a pocket score of 1.87, 9 amino acids, and a probability score of 0.036 (c).

2.30 to -8.60 kcal/mol) with PPARγ (PDB id: 5Y2O). The results revealed that Apigetrin (CID: 5280704), Orientin (CID: 5281675), and Isoquercetin (CID:5280804) showed the highest binding energy of -8.60, -8.50, and -8.30 kcal/mol respectively, against PPARγ (PDB id: 5Y2O). Apigetrin created five hydrophobic interactions and two hydrogen bonds as showed in Figure 3(a) and Table 3, Orientin (CID: 5281675) formed four hydrophobic interactions and seven hydrogen bonds as presented in Figure 3(b) and Table 3, and Isoquercetin (CID: 5280804) formed one hydrophobic and five hydrogen bonds with target protein as depicted in Figure 3(c) and Table 3, between the one of the potential antidiabetic proteins PPARγ.

2.6. Pharmacokinetics and physicochemical evaluations of active molecules

The pharmacokinetic parameters of top-scored bioactive molecules, such as apigenin, orientin, isoquercitrin, and pioglitazone, were assessed by the SwissADME database, and the results are shown in Table 4. All three molecules (except the standard drug pioglitazone) have low gastrointestinal (GI) absorption rates. The bioavailability of apigenin, orientin, isoquercitrin, and pioglitazone was measured as 0.55, 0.17, 0.17, and 0.55, respectively. All three molecules containing the reference drug pioglitazone were reported not to pass the blood-brain barrier (BBB). Table 4 shows that apigenin (432.38 g/mol) violates 1 (NH or OH > 5), orientin (448.38 g/mol) violates 2 (N or O > 10, NH or OH > 5), and isoquercetin (464.38 g/mol) violates 2 (N or O > 10, NH or OH > 5) Lipinski's rule of 5. In contrast, the standard drug pioglitazone, whose molecular weight is 356.44 g/mol, does not violate Lipinski's rule of 5. The bioavailability radar plot demonstrated the drug-like behaviour of the chosen molecules, and the results are shown in Figure 4. Figure 4 depicts an optimal range of active molecules as the pink region within the hexagon. The recommended criteria for a drug-like molecule are: the saturation (SATU) of the carbon fraction in sp^3 hybridization should be no less than 0.25, insolubility (INSOLU) should be at most 6, hydrophobicity (LIPO) should have an XLOGP3 value between -0.7 and +5.0, rotatable bonds (FLEXI) should not exceed nine, molecular weight (SIZE) should be in the range of 150 to 500 g/mol, and the polar surface area (POLAR) should be valued between 20 and 130 $Å^2$. Furthermore, the pharmacokinetic properties of all five selected bioactive compounds and the reference medication were studied using an egg-boiled model, and the findings are reported in Figure 5. The egg-boiled model predicts two key pharmacokinetic characteristics: passive gastrointestinal absorption and blood-brain barrier (BBB) permeability. The egg-shaped organization map shows that albumin (the white area) has extremely high gastrointestinal absorption. In contrast, the chemicals in the yolk (the yellow zone) imply very likely BBB permeability in humans. Figure 6 illustrates that the usual medicine (pioglitazone) and apigetrin has little gastrointestinal absorption. In contrast, the other two molecules (orientin, and isoquercetin) are located out of the egg-boiled graph, indicating that apigenin has the potential to be an effective antidiabetic molecule.

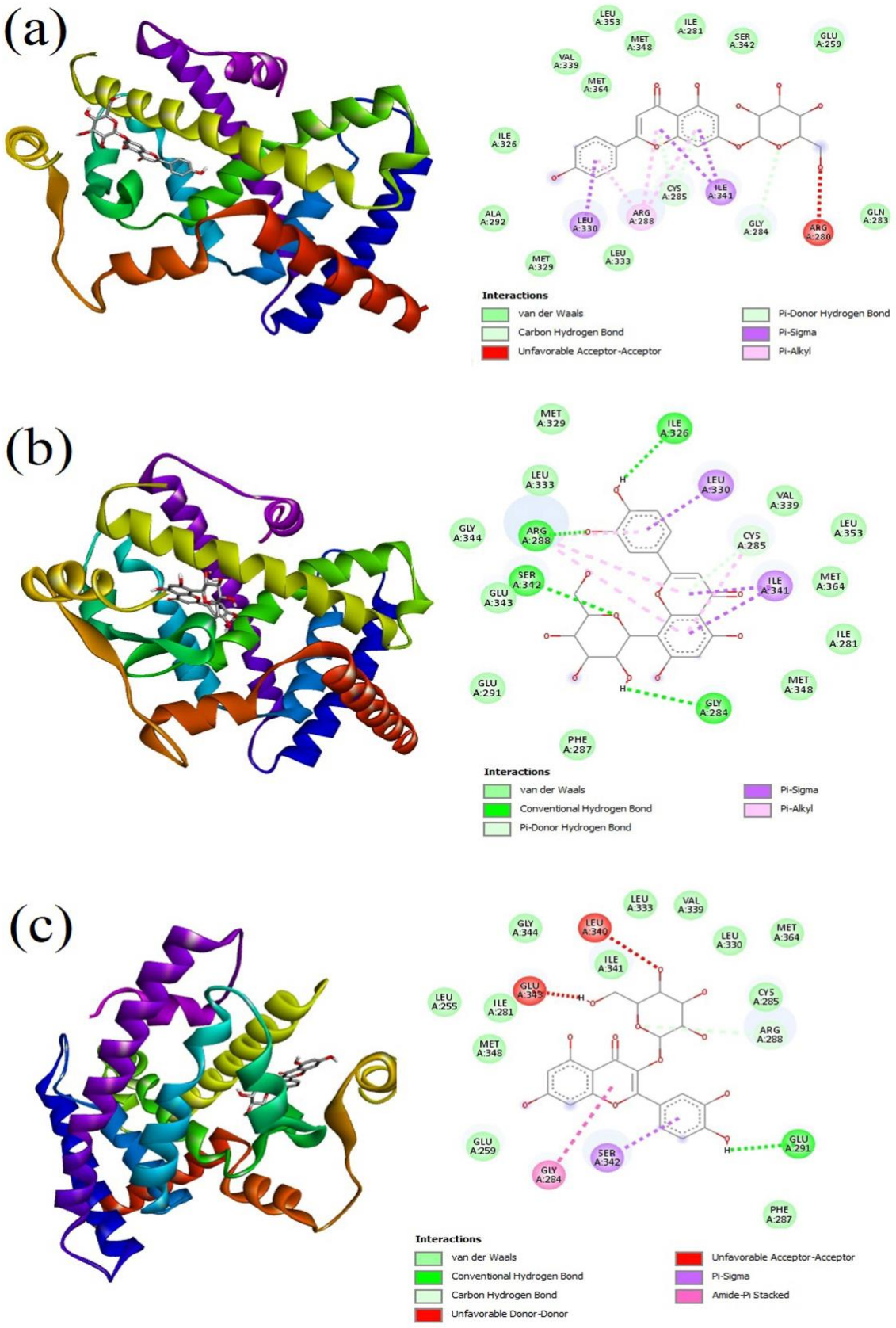

Figure 3. Interaction between the molecule Apigetrin and PPARγ. Left side representing 3D and the right side representing 2D complex protein–ligand interaction (a); the interaction between the molecule Orientin and PPARγ. Left side representing 3D and the right side representing 2D complex protein–ligand interaction (b); and the interaction between the molecule isoquercetin and PPARγ. Left side representing 3D and the right side representing 2D complex protein–ligand interaction (c)

2.7. Toxicity

The online tool Protox-II program assessed the *in-silico* toxicity profile of the outstanding-scoring molecules (apigetrin, orientin, and isoquercetin). Table 5 predicts drug-induced toxicity, hERG, AMES, LD_{50}, skin sensitization, hepatotoxicity, *Tetrahymena pyriformis* (TP), and minnow toxicity. The LD_{50} values of the identified molecules show that the molecules with the lowest toxicity were found to be the most effective in the investigation.

Table 3. List of bonding interactions between selected top-scored bioactive compounds with PPARγ.

Antidiabetic protein receptor	Active molecule	Residue	Amino acid	Distance (Å)	Bond category
PPARγ (PDB id: 5Y2O)	Apigetrin (CID: 5280704)	288A, 288A, 326A, 330A, 341A	ARG, ARG, ILE, LEU, ILE	4.00, 3.40, 3.69, 3.42, 3.53	Hydrophobic
		259A, 288A	GLU, ARG	2.18, 3.34	Hydrogen
	Orientin (CID: 5281675)	288A, 326A, 330A, 341A	ARG, ILE, LEU, ILE	3.31, 3.78, 3.54, 3.52	Hydrophobic
		284A, 288A, 288A, 326A, 343A	GLY, ARG, ARG, ARG, ILE, SER, GLU	2.05, 3.07, 3.12, 2.32, 2.50, 2.25, 2.15	Hydrogen
	Isoquercetin (CID: 5280804)	288A	ARG	3.92	Hydrophobic
		259A, 288A, 291A, 342A, 343A	GLU, ARG, GLU, SER, GLU	2.17, 2.23, 2.26, 2.77, 2.11	Hydrogen

2.8. Molecular dynamics (MD) simulation studies

The MD simulation studies were used to explore the stability of the protein-ligand interactions. MD simulation studies were conducted on the antidiabetic receptor proteins-ligand complexes, including PPARγ-apigetrin, PPARγ-orientin, and PPARγ-isoquercetin. Initially, 10 ns simulation studies were performed for all three complexes to check the stability of the interactions of protein-ligand complexes. PPARγ-isoquercetin has nonstable in the first 10 ns, therefore, we stopped to run further, the other two complexes were highly stable throughout MD simulation studies. The RMSD graph and ligand-protein interactions (2D interaction diagram) were analyzed to provide a comprehensive understanding of the simulated outcomes. The RMSD graphs illustrate the development of the protein (left y-axis) and its ligand (right y-axis). The MD trajectory measures of the docked complex PPARγ-Apigetrin exhibited that the protein root-mean-square deviation (RMSD) between 1.6 Å and 2.3 Å and the ligand RMSD between range from 3.2 and 4.8 Å, demonstrating that it was a stable complex (Figure 6(a)). The MD trajectory events of the docked complex PPARγ-Orientin exhibited that the protein RMSD was between 2.6 and 4.2 Å, while the ligand RMSD ranged from 4.2 and 7.2 Å, indicating the stable complex (Figure 6(b)). Initial 10 ns of MD simulation studies of PPARγ-isoquercetin complex showed a non-stable complex (supplementary Figure 1). The ligands binding to the main functional groups of antidiabetic proteins did not cause any significant alterations in the RMSF analysis of stable two protein-ligand complexes (Figure 7). The PPARγ-apigetrin complex's MD trajectory explored those seven particular amino acids interacting with the recepyor protein. This information was obtained from the residue index, and it was observed that these amino acids did not change during the MD simulation. The PPARγ-orientin complex's MD trajectory indicated a stable relationship between eleven specific amino acids, as evidenced by their residue index and lack of fluctuation during simulation. The critical PPARγ stability and inhibition residues are ARG288, ILE326, and GLU343. The protein-ligand interactions of the PPARγ-apigetrin complex revealed that amino acid residues ARG280

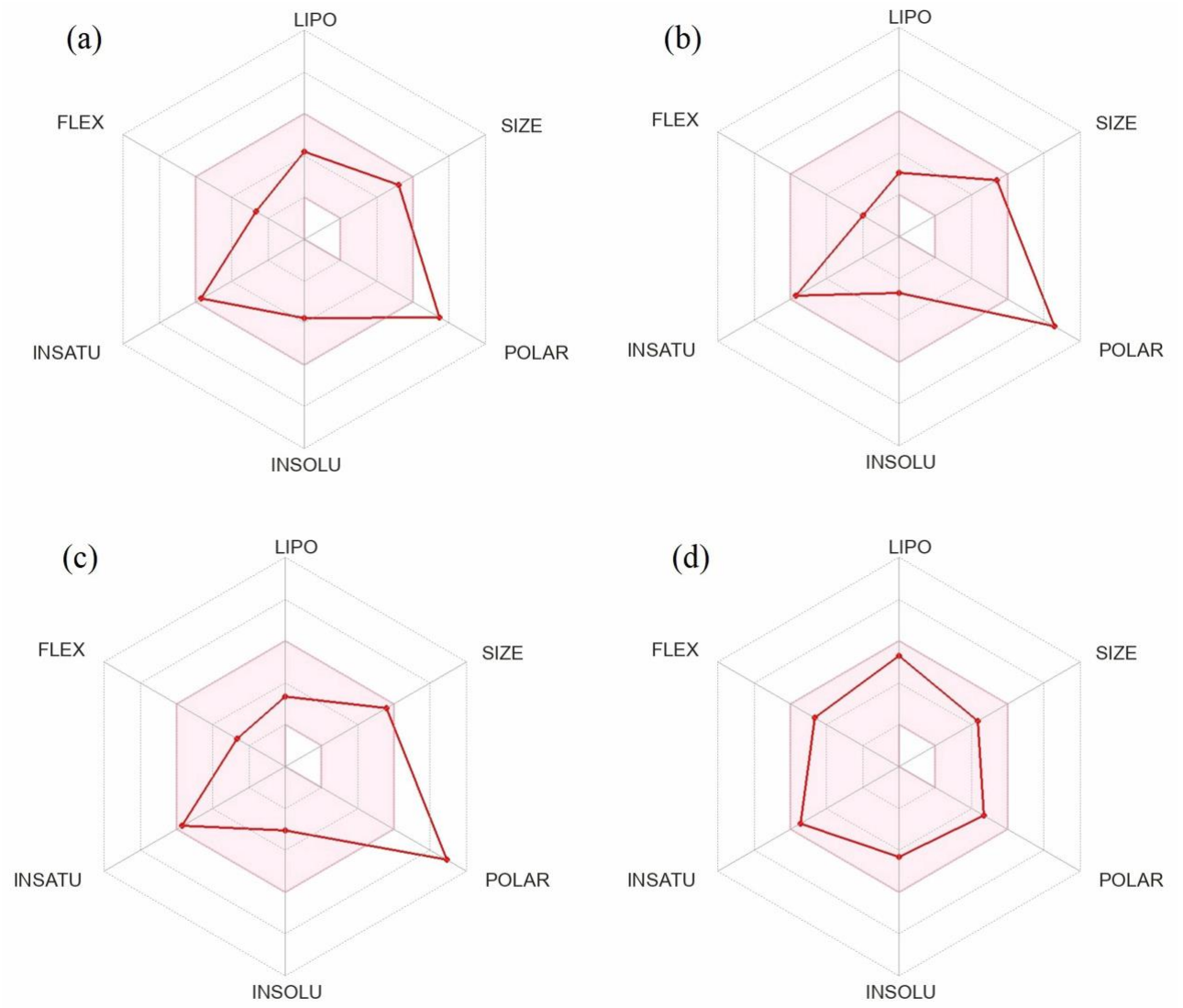

Figure 4. Bioavailability radar plot for oral bioavailability of top-scored active compounds. Apigetrin (a), Orientin (b), Isoquercetin (c), and reference drug (Pioglitazone) (d). the pink area exhibits the optimal range for each property (lipophilicity as XLOGP3 between -0.7 and +5.0; size as molecular weight between 150 and 500 g/mol; polarity as TPSA (topological polar surface area) between 20 and 130 Å2; insolubility in water by log S scale not higher than 6; insaturation as per fraction of carbons in the sp3 hybridization not <0.25 and flexibility as per rotatable bonds no more than 9).

(45%), GLU259 (79%), and LEU225 (32%) contributed the most significant interaction with apigetrin (Figures 8(a), and (b)). The protein-ligand interactions of the PPARγ-orientin complex revealed that amino acid residues GLU291 (56%), LYS263 (33%), and SER342 (33%) contributed the most significant interaction with Orientin (Figure 9(a)and (b)). Figure 10 depict the hydrogen bond interactions as well as chronological representations of all amino acid residues that form H-bonds, hydrophobic, ionic, or water bridges. Darker lines indicate stable interaction with the target. These interactions ensured the protein-ligand combination remained stable throughout the molecular docking simulation studies. *In vitro* study on apigetrin and orientin should be conducted to establish their ability to inhibit PPARγ based on our findings. These molecules could potentially serve as the foundation for future lead optimization.

2.9. DFT

The HOMO is an estimate of a molecule's ability to donate electrons; the frontier-orbital energies (highest occupied molecular orbital (HOMO) and lowest unoccupied molecular orbital (LUMO)) of active molecules have a substantial impact on therapeutic efficacies. The energies and HOMO-LUMO energy gap of selected active molecules apigetrin, orientin, isoquercetin, and reference drug pioglitazone were measured

Table 4. Pharmacokinetics and physicochemical parameters of selected top binding scored bioactive molecule apigetrin, orientin, isoquercetin, and pioglitazone

Parameters	Apigetrin	Orientin	Isoquercetin	Pioglitazone
Formula	$C_{21}H_{20}O_{10}$	$C_{21}H_{20}O_{11}$	$C_{21}H_{20}O_{12}$	$C_{19}H_{20}N_2O_3S$
MW (g mol^{-1})	432.38	448.38	464.38	356.44
Num. heavy atoms	31	32	33	25
Num. aromatic heavy atoms	16	16	16	12
Fraction Csp3	0.29	0.29	0.29	0.32
Num. rotatable bonds	4	3	4	7
Num. H-bond acceptors	10	11	12	4
Num. H-bond donors	6	8	8	1
Molar Refractivity	106.11	108.63	110.16	102.17
TPSA ($Å^2$)	170.05	201.28	210.51	93.59
Solubility	Moderately soluble	Soluble	Moderately soluble	Moderately soluble
GI absorption	Low	Low	Low	High
BBB permeation	No	No	No	No
Violation of Lipinski's rule of five	1 NH or OH>5	2 N or O>10, NH or OH>5	2 N or O>10, NH or OH>5	0
Violation of Veber rule	1 TPSA>140	1 TPSA>140	1 TPSA>140	0
Bioavailability Score	0.55	0.17	0.17	0.55
Synthetic accessibility	5.12	5.17	5.32	3.46

by B3LYP at the 6-311G (d, p) basis set, and the HOMO-LUMO diagrams of apigetrin, orientin, isoquercetin, and pioglitazone are shown in Table 6. The HOMO-LUMO energy gap values for apigetrin, orientin, isoquercetin, and pioglitazone were 3.398432 Δev, 3.258565 Δev, 3.219381 Δev, and 2.734746 Δev, respectively.

3. DISCUSSION

Currently recommended synthetic antidiabetic drugs effectively manage T2DM but cause severe toxic side effects such as hypoglycemia, lactic acidosis risk in patients with provoked unbalanced kidney functions, heart failure, hypoxemia, alcoholism, cirrhosis, contrast exposure, sepsis, shock, gastrointestinal side effects [17]. Plant-derived molecules have provided crucial leads for the development of medicines to treat a variety of diseases. Several studies reported that active plant molecules have a potential antidiabetic efficacy [18]. Plant molecules up or down-regulate the drug receptor proteins to enhance insulin secretion or sensitize the insulin to metabolize the glucose in the circulatory system [19]. The applicability of molecular modeling methods in synthetic medicinal chemistry to plant-derived molecules still needs to be determined and better understood. A few prominent molecules were predicted using *in silico* pharmacoinformatics and confirmed *in vitro* and *in vivo* tests. Pharmacoinformatics is a set of soft-computing tools that allow the molecular structure-based identification of drugs based on binding affinities, pharmacokinetics, and physical properties [20]. Understanding how active substances attach to, interact with, and increase or down-regulate receptor proteins could help researchers create disease treatment options. Our previous study results demonstrated that ethanolic extract of *M. pudica* L. regains body weight, reduces a considerable amount of glucose in the blood, and increases antioxidant enzyme levels in diabetes-induced male rats [16]. Hence, the present study was planned to discover potential antidiabetic molecules and their mechanism of antidiabetic efficacy from *M. pudica* L.

The plant *M. pudica* L. traditionally used for numerous health complications and possesses several pharmacologically active molecules, particularly L-mimosine, stigmasterol, isoorientin, vitexin, cassiaoccidentalin B, isovitexin, apigetrin, isoquercetin, avicularin, beta-sitosterol, methyl quercetin, orientin,

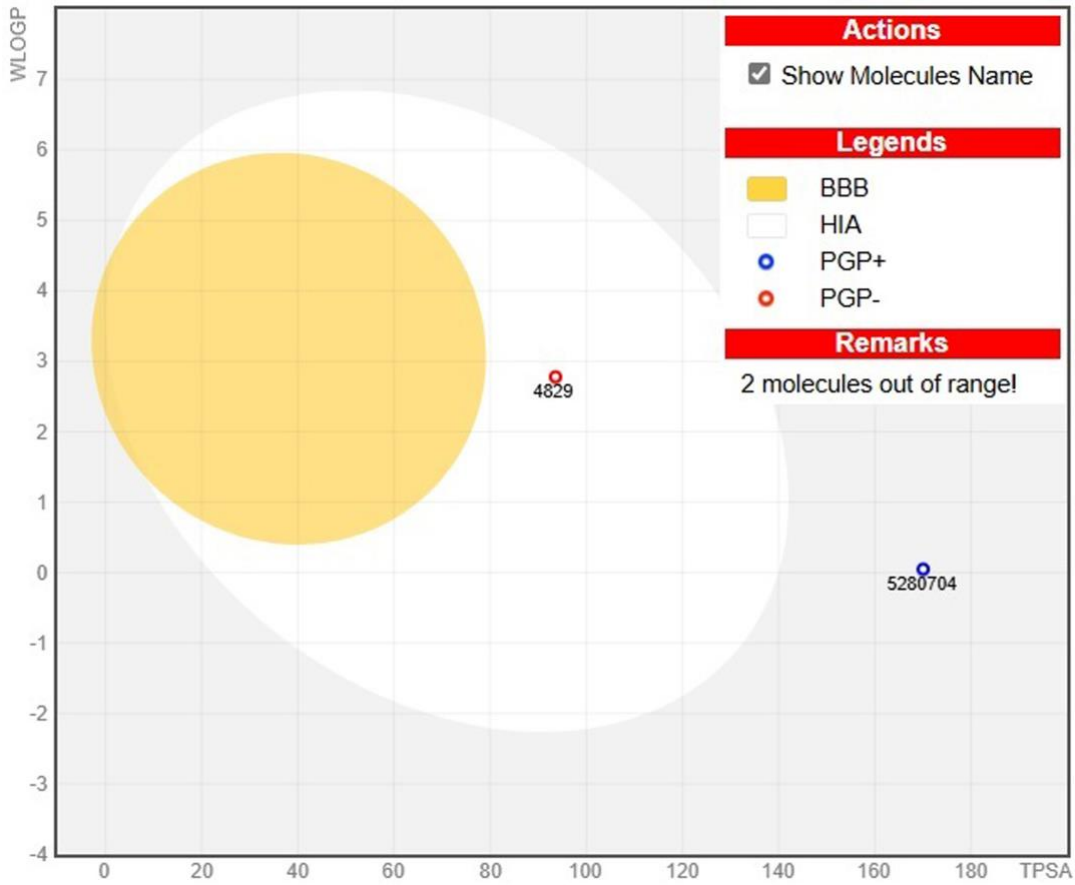

Figure 5. The EGG-BOILED model for the top-scored active molecules and reference drug pioglitazone. The EGG-BOILED represents for intuitive evaluation of passive gastrointestinal absorption (HIA) white part and brain penetration (BBB) yellow part as well as substrates (PGP-) and non-substrates (PGP+) of the permeability glycoprotein (PGP) are represented by blue and red colour circles, respectively, of the selected active molecules and reference drug pioglitazone in the WLOGP-vs.-TPSA graph. The grey region is the physicochemical space of molecules predicted to exhibit high intestinal absorption.

betulinic acid, abscisic acid, etc. [21], In advanced *in silico* molecular modeling tools are used to identify potential molecules based on their binding affinities against one of the antidiabetic protein receptors, PPARγ. Precise prediction of drug-target interactions can help guide the drug discovery process and accelerate drug development. In this study, a potential antidiabetic drug receptor was identified from the signaling pathway of T2DM through graph theoretical network analysis. The developing graph theoretical network has been swiftly deployed to predict drug-target interactions, proving helpful in repositioning drugs and speeding up drug discovery. The nuclear Peroxisome proliferator-activated receptors (PPARα, PPARβ/δ, and PPARγ) act as transcription factors to regulate several physiological functions via ligand activation [22]. PPARγ-activating molecules improve insulin sensitivity and glucose metabolism. PPARγ is predominantly expressed in endothelial and vascular smooth muscle cells. In our earlier investigation, we detected thirty-six active molecules in an ethanolic extract of *M. pudica* L. using gas chromatography-mass and liquid chromatography-mass spectroscopy analysis. The discovered compounds bind to PPARγ, an antidiabetic protein receptor, with binding energy ranging from -2.4 to -8.6 kcal/mol. Three compounds, apigetrin (-8.6 kcal/mol), orientin (-8.5 kcal/mol), and isoquercetin (-8.3 kcal/mol), demonstrated substantial hydrogen bonding and hydrophobic interactions with the PPARγ.

Therapeutic efficacy mainly depends on plant-derived molecules' pharmacokinetic (ADME), physicochemical, and pharmacodynamic properties [23]. The pharmacokinetic process of a drug is whether a drug can get to the site of action. To understand pharmacodynamic qualities, it is required to assess molecules' bioavailability at the target site, and their absorption and metabolism within the human body [24]. As a result, plant-derived molecules with lower pharmacokinetics capability and toxic properties

Table 5. List of the drug-induced hERG inhibition, AMES toxicity, carcinogens, Tetrahymena pyriformis (TP) toxicity, rat acute toxicity (LD50 in mol kg-1), and skin sensitisation along with Minnow toxicity of apigetrin, orientin, isoquercetin, and pioglitazone.

Parameters	Apigetrin	Orientin	Isoquercetin	Pioglitazone
AMES toxicity	No	Yes	Yes	No
Max. tolerated dose (human) (log mg/kg/day)	0.698	0.814	0.508	0.416
hERG inhibition	No	No	No	No
Oral Rat Acute Toxicity LD_{50} (mol kg^{-1})	2.689	2.915	2.624	2.25
Hepatotoxicity	No	No	No	Yes
Oral Rat Chronic Toxicity (LOAEL) (log mg/kg b.w/day)	2.442	3.657	4.07	1.775
Skin Sensitisation	No	No	No	No
T. pyriformis toxicity (log ug L^{-1})	0.285	0.285	0.285	1.07
Minnow toxicity (log mM)	1.131	3.712	2.706	-0.113

should be avoided during drug discovery, as natural substances must be therapeutically helpful and have crucial pharmacokinetic characteristics [25]. Various plant-derived molecules are to be investigated at this stage, but physical samples are scarce. As a result, computer-assisted modeling techniques offer a viable alternative to animal testing. Lipinski's rule of five is a widely utilized drug-likeness property of phytoconstituents that predicts a phytocompounds capacity to be orally active in the human body. This research focused on the *in silico* toxicity prediction methods to assess the toxicity levels of five high-scoring chemicals. The three highest-scoring active compounds passed all toxicity experiments (hERG toxicity, carcinogenicity, skin irritation, and acceptable logBB values). Finally, MD simulation experiments were performed to explore protein-ligand complexes' intermolecular interactions and stability. ARG280, ARG288, GLU259, and GLU343 are critical residues stabilizing ligand binding and decreasing PPARγ activity. The crucial amino acid interaction occurs via hydroxy substitution. Apigetrin and orientin are promising candidates for inhibiting PPARγ; further *in vitro* and *in vivo* experiments must be confirmed.

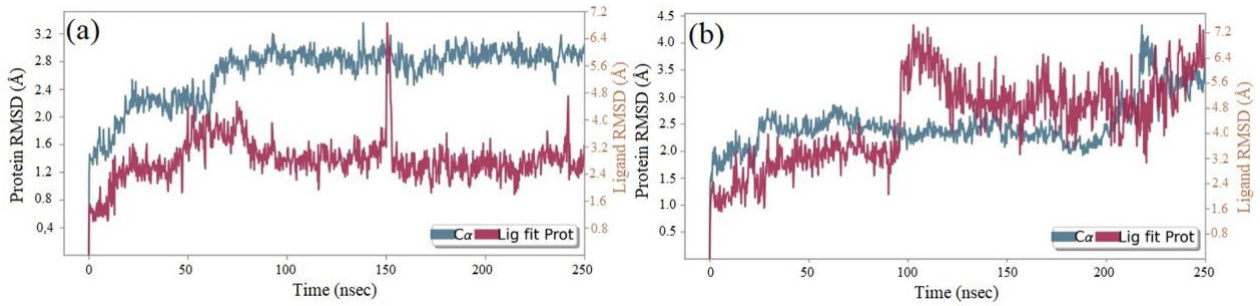

Figure 6. RMSD study plot for 250ns MD simulation of Apigetrin-PPARγ docked complex (a), Orientin-PPARγ docked complex (b).

Table 6. E_{HOMO} and E_{LUMO} and Δev values of selected top binding scored compounds, apigetrin, orientin, isoquercetin and standard drug pioglitazone.

Compound	HOMO	E_{HOMO} (ev)	LUMO	E_{LUMO} (ev)	Energy gap (Δev)
Apigetrin	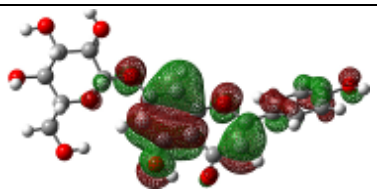	-0.32895	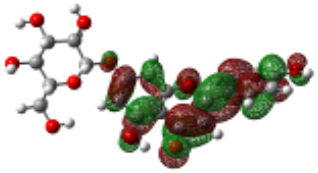	-0.20406	3.398432
Orientin	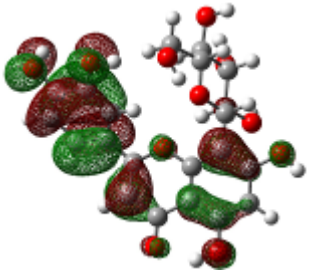	-0.32277	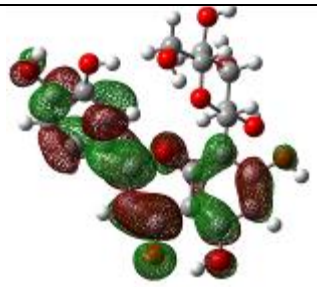	-0.20302	3.258565
Isoquercetin	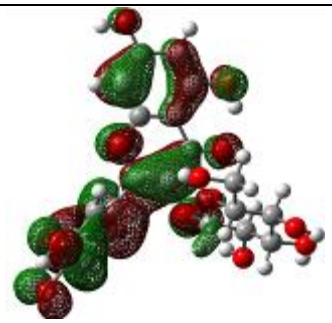	-0.31796	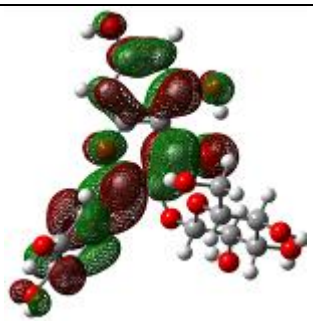	-0.19965	3.219381
Pioglitazone	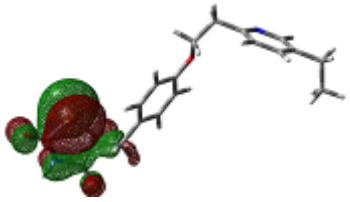	-0.29364	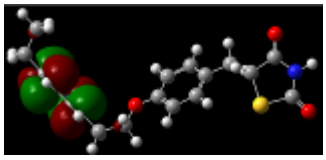	-0.19314	2.734746

4. CONCLUSION

Plant-derived molecules demonstrated significant therapeutic benefits in preventing various human disorders/diseases. They are safe, have little toxicity, and are a cost-effective medicine that enhances the quality of life. Our earlier investigation found that an *M. pudica* L. extract enhances the aphrodisiac efficiency in diabetes-induced male Wistar rats while reducing diabetic complications. This study predicted active molecules in the ethanolic extract of *M. pudica* L. against T2DM. PPARγ was identified as a possible antidiabetic target by graph theoretical network research. PPARγ inhibitors lower HbA1c levels and improve insulin sensitivity in T2DM. *In silico* molecular docking studies showed that apigetrin, orientin, and isoquercetin had the most significant binding score against the PPARγ receptor protein. Further, *in silico* pharmacokinetic, physicochemical, and toxicity analyses reveal a harmless profile for all three top-scored molecules. MD simulation studies show that apigenin and orientin interact and stabilize with the PPARγ receptor protein. Additionally, *in vitro* cellular and *in vivo* animal studies are needed to assess the antidiabetic potential of these molecules from *M. pudica* L.

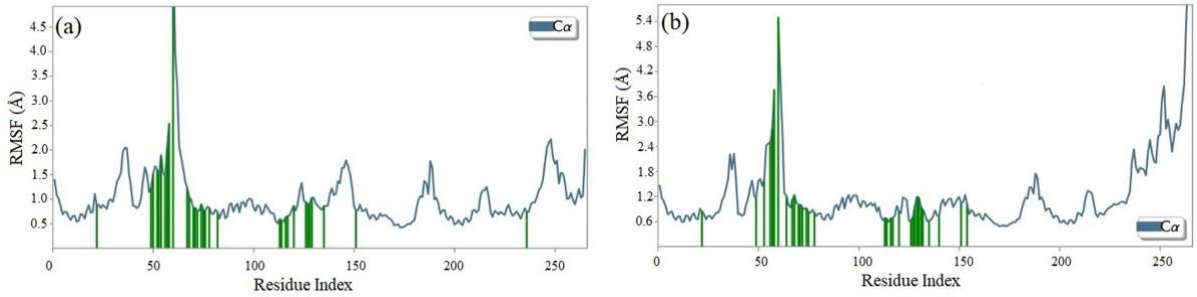

Figure 7. Root mean square fluctuation (RMSF) of the Apigetrin for characterizing changes in the ligand atom positions (a), root mean square fluctuation of the Orientin for characterizing changes in the ligand atom positions (b).

5. MATERIALS AND MTHODS

5.1. Antidiabetic molecules prediction

A total of thirty-six active molecules from *M. pudica* L. were identified based on the results of our previously published work, and they are presented in Table 1. For structure-based molecular prediction against one of the potential antidiabetic receptor proteins, the identified molecule's structure was drawn by ACD/Chemsketch online software v. 2021.2.2 and saved in SDF format (Structure Data File). BIOVIA Discovery Studio software was employed to generate the cluster molecule library that is ready to dock. Initially, the energy of the selected molecules was minimized by using the Avogadro software tool (https://avogadro.cc/; accessed on May 2nd, 2024), and the molecules were converted into the '.PDBQT' format by using the Open Babel tool (https://openbabel.org/; accessed on May 2nd, 2024).". Receptor Protein Preparation: The X-ray crystallographic structure of the PPARγ ligand binding domain-pioglitazone complex (PDB id: 5Y2O, Homo sapiens, Resolution: 1.80 Å) was obtained from RCSB PDB (https://www.rcsb.org/structure/5Y2O) webpage. The Swiss-PDB visualized softwarev.4.1.0 was used to eliminate water ions, co-crystallized ligands, and other unnecessary components from the protein. It also added missing residues to the recovered protein. The file was saved as targetor.pdb' in the .pdb format. Additionally, we used BIOVIA Discovery Studio Visualizer v.4.0 (Accelrys, Inc., San Diego, California, United States America) to illustrate the target protein structure and arrangement of amino acids from active pockets, which were then used in molecular docking investigations [26].

5.2 Ligand binding site identification

Identifying the ligand binding sites within a specific protein region has several practical applications for understanding protein function and structure-based drug discovery. This binding site prediction enables active compounds to bind and establish sufficient contact with the target protein, resulting in a solid ligand-target site interaction that provides optimal and beneficial catalytic effects. The probable binding sites of the intended active compounds were identified using the PrankWeb online tool (https://prankweb.cz/; evaluated on May 16th, 2024) for future exploration [21]. The PyRx algorithm built a receptor grid box after predicting the target protein's active binding location.

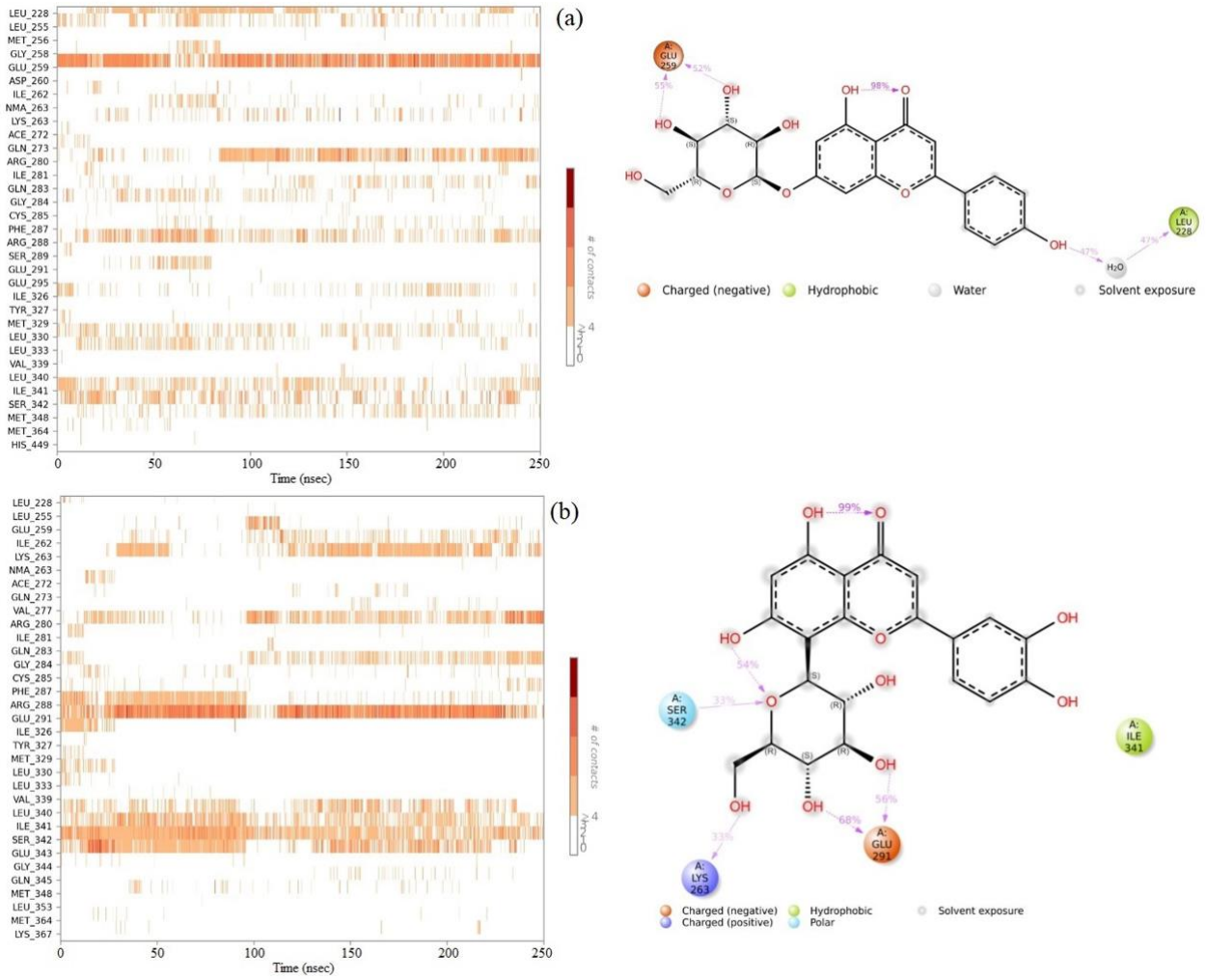

Figure 8. PPARγ-Apigetrin docked complex timeline representation of the Apigetrin (right side) contacts with respect to the amino acids in the target (left side) (a). PPARγ-Orientin docked complex timeline representation of the Apigetrin (right side) contacts with respect to the amino acids in the target (left side) (b).

5.3 *In silico* docking analysis

The PyRx 0.8 virtual tool in the AutoDock Vina application investigated the *in silico* molecular docking of selected molecules against PPARγ, a potential antidiabetic receptor protein (PDB ID: 5Y2O). The protein and active molecules files were saved in the ".pdbqt" format to calculate molecular binding affinities (kcal/mol). A grid box with a radius of 10.0 Å was created to reflect the estimated region of active binding sites. The AutoDock Vina program compared the binding energy affinities of up to ten docking sites per ligand. All complex binding bond affinity energies were estimated using the ligand conformation at the active binding bond, taking into account the RMSD (root mean square deviation) between the original and subsequent structures. The number of hydrogen bonds and non-covalent interactions in each protein-ligand complex were displayed using Discovery Studio Visualizer, which produced the details of interaction images (2D and 3D structure) [27].

5.4 Physicochemical, drug-likeness, pharmacokinetic and toxicity studies

We observed the drug-like properties and resilience of the top-scoring active molecules utilizing *in silico* ADME (absorption, distribution, metabolism, and excretion) studies as well as physicochemical features. The SwissADME web service (http://www.swissadme.ch/; evaluated by June 6th, 2024) looked at molecular weight, molar refractivity, water solubility, bioavailability, and other factors like radar maps, the egg-boiled model, brain penetration, and human gastrointestinal absorption. The free SwissADME program enables researchers to assess the pharmacokinetic properties and drug-likeness of test chemicals and

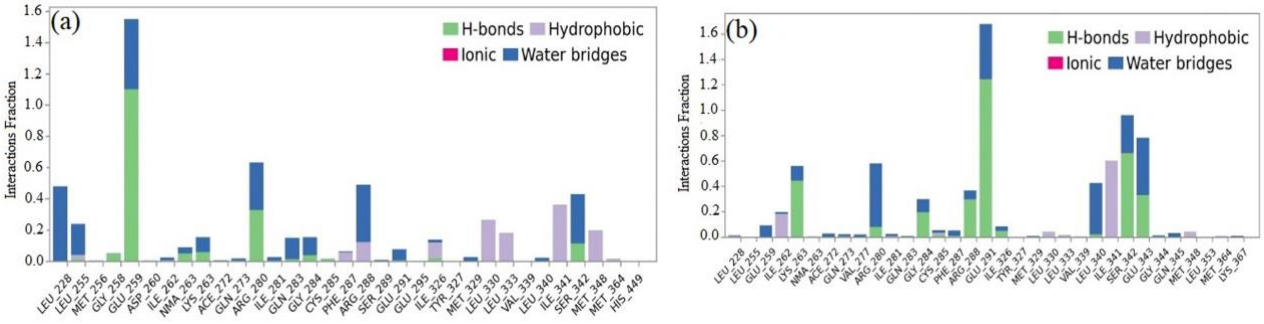

Figure 9. Percentage of amino acid and water-mediated interactions in MD simulations with Apigetrin (a), and Orientin (b).

reference medications [28]. The Protox-II web tool (https://tox-new.charite.de/protox_II/; assessed by June 10th, 2024) was used to predict the toxicity profile of active molecules [29].

5.5. Molecular dynamics (MD) simulation studies

Molecular dynamics (MD) simulation assessed the outstanding -scored three ligands with the most excellent docking binding scores of antidiabetic protein receptor-ligand complexes using the DESMOND dynamic package 2017 to investigate protein-ligand complexes' stability and intermolecular interactions (PLC) [30]. MD simulation modeling demonstrates the prominent effects of PLC on target binding sites in physiological conditions. On a Linux platform, the dependent on-time development of the complexes was calculated over 250 nanoseconds. To simulate, the complex was centered in an orthorhombic cubic box with TIP3P water molecules and buffers positioned 10 Å from the box edge and protein atom [31]. Panel of System Developers: Initially, the panel creates a box (10 × 10 × 10) with water models and physiological environments like pH. If pH is not present or must be altered to fit study conditions, Na+ or Cl- ions can be added. The docked protein-ligand complexes were solved using the SPC water model. Counter ions neutralize the solution while keeping the physiological salt concentration at 0.15 M. The protein-ligan complex system was evaluated using the OPLS AA (Optimal Potentials for Liquid Simulation - All Atom) force field [32]. The system builder panel will conduct a mild minimization on the ready PLC at around 100 picoseconds. In molecular dynamics with relaxation durations of two picoseconds, the integrator of the reversible Reference System Propagator Algorithms (RESPA), the Martyna-Tobias-Klein barostat, and the Nose-Hoover chain thermostat have all been applied [33, 34]. The MD simulation for 250 ns was performed using the NPT ensemble with the default relaxation settings at 310.15 K temperature and 1.0 bar pressure [35]. Following the simulation, the results were analyzed using a simulation interaction diagram.

5.6. Analysis of DFT

The DFT has emerged as an effective tool for sensing and predicting the antidiabetic potential of molecules. DFT's primary purpose is to offer quantitative information about material properties by applying fundamental quantum mechanics concepts. This work used molecular docking to identify the top binding-score active molecules, and computational measurements were carried out using the Gaussian 03W software and the GaussView molecular visualization tool. The molecular structures of the discovered active molecule were optimized using the DFT/Becke-3-Lee-Yang-Parr (B3LYP) method on a 6-311G (d.p) basis set [20]. The optimized structures were utilized to calculate the frontier molecular orbital energies of the chosen bioactive chemicals. GaussView, a molecular visualization program, presented the molecular orbital energy diagrams for the selected bioactive molecules.

Acknowledgements: CP, MS and SK gratefully acknowledge the Management of Kalasalingam Academy of Research and Education for Seed Money Grant (KARE/VC/R&D/SMPG/2021–2022/1).
Author contributions: Concept – C.P., P.P., S.K.; Design – C.P., M.S., A.K.; Supervision – S.K.; Resources – K.S., T.P.; Materials: C.P., P.P., S.K.; Data Collection and/or Processing – C.P., P.P. S.K.; Analysis and/or Interpretation – C.P., P.P., T.P., M.S., A.K.; Literature Search – C.P., P.P., P.P., T.P., M.S., A.K, S.K.; Writing –C.P.; Critical Reviews – C.P., P.P., T.P., M.S., A.K..
Conflict of interest statement: The authors report no financial interest that might pose a potential, perceived or real conflict of interest.

REFERENCES

[1] Meetoo D, McGovern P, Safadi R. An epidemiological overview of diabetes across the world. Br J Nur. 2007; 16: 1002-1007. https://doi.org/10.12968/bjon.2007.16.16.27079

[2] Chávez-Reyes J, Escárcega-González CE, Chavira-Suárez E, León-Buitimea A, Vázquez-León P, Morones-Ramírez JR, Villalón CM, Quintanar-Stephano A, Marichal-Cancino BA. Susceptibility for some infectious diseases in patients with diabetes: The key role of glycemia. Front Public Health. 2021; 9: 559595. https://doi.org/10.3389/fpubh.2021.559595

[3] Leggio M, Lombardi M, Caldarone E, Severi P, D'emidio S, Armeni M, Bravi V, Bendini MG, Mazza A. The relationship between obesity and hypertension: an updated comprehensive overview on vicious twins. Hypertens Res. 2017; 40: 947-963. https://doi.org/10.1038/hr.2017.75

[4] Pradeepa R, Mohan V. Epidemiology of type 2 diabetes in India. Ind J Ophthalmol. 2021; 69: 2932-2938. https://doi.org/10.4103/ijo.ijo_1627_21

[5] Kunjiappan S, Panneerselvam T, Prasad P, Sukumaran S, Somasundaram B, Sankaranarayanan M, Murugan I, Parasuraman P. Design, graph theoretical analysis and in silico modeling of *Dunaliella bardawil* biomass encapsulated keratin nanoparticles: A scaffold for effective glucose utilization. Biomed Mat. 2018; 13: 045012. http://dx.doi.org/10.1088/1748-605X/aabcea.

[6] Kim J, Kwon HS. Not control but conquest: strategies for the remission of type 2 diabetes mellitus. Diabet Metabolism J. 2022; 46: 165-180. https://doi.org/10.4093/dmj.2021.0377

[7] Martín-Timón I, Sevillano-Collantes C, Segura-Galindo A, del Cañizo-Gómez FJ. Type 2 diabetes and cardiovascular disease: have all risk factors the same strength? World J Diabet. 2014; 5: 444. https://doi.org/10.4239%2Fwjd.v5.i4.444

[8] Das SK, Chakrabarti R. Non-insulin dependent diabetes mellitus: Present therapies and new drug targets. Mini Rev Med Chem. 2005; 5: 1019-1034. https://doi.org/10.2174/138955705774575273

[9] Artasensi A, Pedretti A, Vistoli G, Fumagalli L. Type 2 diabetes mellitus: A review of multi-target drugs. Molecules. 2020; 25: 1987. https://doi.org/10.3390/molecules25081987

[10] Al-Mrabeh A. β-Cell dysfunction, hepatic lipid metabolism, and cardiovascular health in type 2 diabetes: new directions of research and novel therapeutic strategies. Biomedicines. 2021;9(2):226. https://doi.org/10.3390/biomedicines9020226

[11] Dinda B, Saha S. Obesity and Diabetes. In Natural Products in Obesity and Diabetes: Therapeutic Potential and Role in Prevention and Treatment; Springer: 2022; pp. 1-61.

[12] Kunjiappan S, Theivendren P, Pavadai P, Govindaraj S, Sankaranarayanan M, Somasundaram B, Arunachalam S, Ram Kumar Pandian S, Ammunje DN. Design and in silico modeling of indoloquinoxaline incorporated keratin nanoparticles for modulation of glucose metabolism in 3T3-L1 adipocytes. Biotechnol Prog. 2020; 36: e2904. https://doi.org/10.1002/btpr.2904

[13] Savinell JM, Palsson BO. Network analysis of intermediary metabolism using linear optimization. I. Development of mathematical formalism. J Theor Biol. 1992; 154: 421-454. https://doi.org/10.1016/s0022-5193(05)80161-4

[14] Shao X, Wang M, Wei X, Deng S, Fu N, Peng Q, Jiang Y, Ye L, Xie J, Lin Y. Peroxisome proliferator-activated receptor-γ: master regulator of adipogenesis and obesity. Curr Stem Cell Res Ther. 2016; 11: 282-289. https://doi.org/10.2174/1574888x10666150528144905

[15] Muhammad G, Hussain MA, Jantan I, Bukhari SNA. *Mimosa pudica* L., a high-value medicinal plant as a source of bioactives for pharmaceuticals. Compr Rev Food Sci Food Saf. 2016; 15: 303-315. https://doi.org/10.1111/1541-4337.12184

[16] Palanichamy C, Nayak Ammunje D, Pavadai P, Ram Kumar Pandian S, Theivendren P, Kabilan SJ, Babkiewicz E, Maszczyk P, Kunjiappan S. Mimosa pudica Linn. extract improves aphrodisiac performance in diabetes-induced male Wister rats. J Biomol Struct Dyn. 2025;43(4):1621-1640. https://doi.org/10.1080/07391102.2023.2292302

[17] Chaudhury A, Duvoor C, Reddy Dendi VS, Kraleti S, Chada A, Ravilla R, Marco A, Shekhawat NS, Montales MT, Kuriakose K. Clinical review of antidiabetic drugs: Implications for type 2 diabetes mellitus management. Front Endocrinol. 2017; 8: 6. https://doi.org/10.3389%2Ffendo.2017.00006

[18] Ansari P, Akther S, Hannan J, Seidel V, Nujat NJ, Abdel-Wahab YH. Pharmacologically active phytomolecules isolated from traditional antidiabetic plants and their therapeutic role for the management of diabetes mellitus. Molecules. 2022; 27: 4278. https://doi.org/10.3390%2Fmolecules27134278

[19] Shehadeh MB, Suaifan GA, Abu-Odeh AM. Plants secondary metabolites as blood glucose-lowering molecules. Molecules. 2021; 26: 4333. https://doi.org/10.3390/molecules26144333

[20] Kalimuthu AK, Panneerselvam T, Pavadai P, Pandian SRK, Sundar K, Murugesan S, Ammunje DN, Kumar S, Arunachalam S, Kunjiappan S. Pharmacoinformatics-based investigation of bioactive compounds of Rasam (South Indian recipe) against human cancer. Sci Rep. 2021; 11: 21488. https://doi.org/10.1038/s41598-021-01008-9

[21] Palanichamy C, Pavadai P, Panneerselvam T, Arunachalam S, Babkiewicz E, Ram Kumar Pandian S, Shanmugampillai Jeyarajaguru K, Nayak Ammunje D, Kannan S, Chandrasekaran J. Aphrodisiac performance of bioactive compounds from *Mimosa pudica* Linn.: In silico molecular docking and dynamics simulation approach. Molecules. 2022; 27: 3799. https://doi.org/10.3390/molecules27123799

[22] Houseknecht KL, Cole BM, Steele PJ. Peroxisome proliferator-activated receptor gamma (PPARγ) and its ligands: a review. Domest Anim Endocrinol. 2002; 22: 1-23. https://doi.org/10.1016/S0739-7240(01)00117-5
[23] Anwar N, Teo YK, Tan JBL. The role of plant metabolites in drug discovery: Current challenges and future perspectives. In: Natural Bio-active Compounds: Volume 2: Chemistry, Pharmacology and Health Care Practices. Springer, Singapore, 2019, pp.25-51. https://doi.org/10.1007/978-981-13-7205-6_2.
[24] Benet LZ, Kroetz D, Sheiner L, Hardman J, Limbird L. Pharmacokinetics: the dynamics of drug absorption, distribution, metabolism, and elimination. In: Goodman and Gilman's the Pharmacological Basis of Therapeutics, 9th Edition. Mcgraw-Hill, New York, 1996, 3, e27.
[25] Dehelean CA, Marcovici I, Soica C, Mioc M, Coricovac D, Iurciuc S, Cretu OM, Pinzaru I. Plant-derived anticancer compounds as new perspectives in drug discovery and alternative therapy. Molecules. 2021; 26: 1109. https://doi.org/10.3390/molecules26041109
[26] Daniel DJP, Shanmugasundaram S, Chandra Mohan KS, Siva Bharathi V, Abraham JK, Anbazhagan P, Pavadai P, Ram Kumar Pandian S, Sundar K, Kunjiappan S. Elucidating the role of phytocompounds from *Brassica oleracea* var. italic (Broccoli) on hyperthyroidism: an in-silico approach. In Silico Pharmacol. 2024; 12: 6. https://doi.org/10.1007/s40203-023-00180-2
[27] Chandrasekaran J, Elumalai S, Murugesan V, Kunjiappan S, Pavadai P, Theivendren P. Computational design of PD-L1 small molecule inhibitors for cancer therapy. Mol Divers. 2023; 27: 1633-1644. https://doi.org/10.1007/s11030-022-10516-3
[28] Daina A, Michielin O, Zoete V. SwissADME: a free web tool to evaluate pharmacokinetics, drug-likeness and medicinal chemistry friendliness of small molecules. Sci Rep. 2017; 7: 42717. https://doi.org/10.1038/srep42717
[29] Pampalakis G. Underestimations in the In Silico-Predicted Toxicities of V-Agents. J Xenobiotics. 2023; 13: 615-624. https://doi.org/10.3390%2Fjox13040039
[30] Prieto-Martínez FD, Galván-Ciprés, Y. Colín-Lozano, B. Molecular simulation in drug design: An overview of molecular dynamics methods. In: Applied Computer-Aided Drug Design: Models and Methods, 2023, p.202. https://doi.org/10.2174/9789815179934123010009
[31] Gopinath P, Kathiravan, M. Docking studies and molecular dynamics simulation of triazole benzene sulfonamide derivatives with human carbonic anhydrase IX inhibition activity. RSC Adv. 2021; 11: 38079-38093. https://doi.org/10.1039/D1RA07377
[32] Espinosa JR, Wand CR, Vega, C. Sanz, E. Frenkel, D. Calculation of the water-octanol partition coefficient of cholesterol for SPC, TIP3P, and TIP4P water. J Chem Phy. 2018; 149. https://doi.org/10.1063/1.5054056
[33] Lippert RA, Predescu C, Ierardi DJ, Mackenzie KM, Eastwood MP, Dror RO, Shaw DE. Accurate and efficient integration for molecular dynamics simulations at constant temperature and pressure. J Chem Phy. 2013; 139. https://doi.org/10.1063/1.4825247
[35] Janek J, Kolafa J. Novel barostat implementation for molecular dynamics. J Chem Phy. 2024; 160. https://doi.org/10.1063/5.0193281
[36] Piston K. Atomistic Investigation of Nucleosomal H3 Histone Tail in Unmodified and Epigenetically Modified States. Syracuse University, 2022.